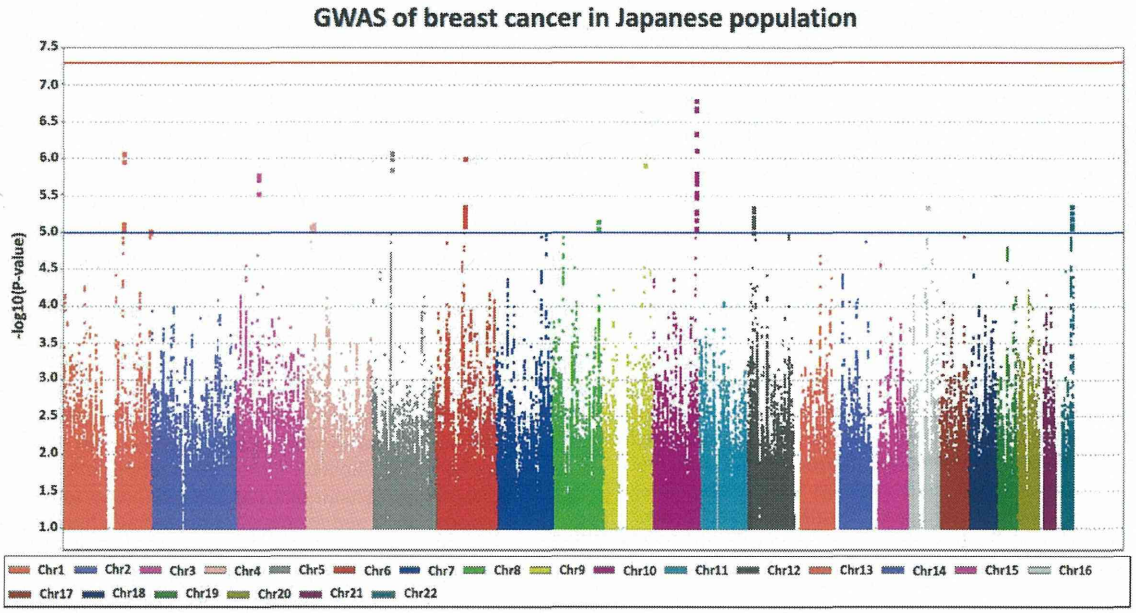

Figure 1. The Manhattan plot for GWAS of breast cancer in the Japanese population. This plot is based on $-\log_{10}$ (*P*-value) from GWAS and imputation analysis against chromosome position, each color represents different chromosome. Blue line indicate suggestive association threshold, $P=1\times10^{-5}$ while red line indicate genome-wide significant threshold $P<5\times10^{-8}$.
doi:10.1371/journal.pone.0076463.g001

Imputation analysis

To increase the power and coverage of the genome-wide association scan, we performed whole genome imputation using 1000G of East Asian population (Japanese in Tokyo JPT, Chinese in Beijing CHB and Chinese in Denver CHD) Phase I Integrated Release Version 2 dataset as reference panel to infer missing genotypes. Briefly, we prepared the input files after quality control, which excluded SNPs with genotyping rate of $\leq$98%, those that deviated from HWE (HWE $P\leq1.0\times10^{-6}$) and those with MAF of $<$0.01. We then confirmed that the allele frequencies of the reference allele are comparable between the GWAS dataset and the reference panel with differences of $<$0.15. By using MACH1.0 (http://www.sph.umich.edu/csg/abecasis/MACH/index.html), we performed haplotype phasing with the samples' genotypes referring 1000G reference panel, estimated the map crossover and error rates using 20 iterations of the Markov chain. Subsequently, we imputed the missing genotypes using Minimac (http://genome.sph.umich.edu/wiki/Minimac). We utilized stringent imputation quality control by excluding SNPs with r^2 value of $<$0.9.

Validation study

After evaluating the associations from GWAS and whole genome imputation, we selected a total of 13 candidate loci that showed suggestive association ($P<1.0\times10^{-5}$) with breast cancer risk for further validation by an independent set of 2,885 cases and 3,395 controls. We genotyped the cases with the multiplex-PCR Invader assay [36] and the control samples with either Illumina OmniExpress BeadChip Kits or by imputation. To verify the accuracy of the imputation analysis, we also included surrogate SNPs that showed close link ($r^2>0.8$ and D' = 1.00) to the imputed SNPs and were included in the genotype platform. Considering multiple testing at this validation stage, we applied Bonferroni significance threshold at $P<3.85\times10^{-3}$ (0.05/13 independent tests).

Evaluation of previously reported loci

To verify previously-reported loci showing the association with breast cancer in the European and East Asian populations, we evaluated 67 loci in the current Japanese GWAS dataset [18–34]. Among the 67 SNPs examined, 6 SNPs are not polymorphic in the Japanese population, 26 SNPs are same as the previously-reported SNPs, 33 and 2 SNPs are SNPs having r^2-value of more than 0.8 and 0.7 to the previously-reported SNPs, respectively (Table S4).

Statistical Analysis

The case-control associations of the GWAS discovery set and validation set were evaluated using logistic regression analysis after considering age as confounding factor from PLINK software (http://pngu.mgh.harvard.edu/~purcell/plink/). The associations of the imputed SNPs were generated with mach2dat software which utilized the output results from Minimac (dosage of the imputed SNP). To have an overview of the association of SNPs with breast cancer, a Manhattan plot of the study was plotted using Haploview 4.1. Meta-analysis for the combined analysis of the discovery and validation phase was performed using inverse-variance method and heterogeneity between the two phases was evaluated using Cochran's Q test. Regional association plots were

Table 2. Association study of SNPs on chromosome 10q26.13 and 16q12.1.

CHR	SNP	BP	Stage	RA	NRA	NCASES	NCONTROLS	RAF_Case	RAF_Ctrl	P_value	OR	SE	L95	U95	P_hetero	*Gene*	rel.loci
10	rs2981578	123340311	GWAS	C	T	2642	2097	0.571	0.517	2.25E-07	1.238	0.041	1.142	1.342		*FGFR2*	0
10	rs2981578	123340311	Rep	C	T	2883	3395	0.556	0.512	1.63E-06	1.213	0.040	1.121	1.313			
10	rs2981578	123340311	Combined	C	T	5525	5492	0.563	0.514	1.31E-12	1.225	0.028	1.158	1.296	7.18E-01		
16	rs12922061	52635000	GWAS	T	C	2641	2099	0.287	0.245	4.50E-06	1.244	0.048	1.133	1.365		*LOC643714*	0
16	rs12922061	52635000	Rep	T	C	2880	3395	0.278	0.239	1.41E-05	1.219	0.046	1.115	1.333			
16	rs12922061	52635000	Combined	T	C	5521	5494	0.282	0.241	3.97E-10	1.231	0.032	1.153	1.314	7.60E-01		
Another SNP on 16p12 that independently associated with breast cancer																	
16	rs3803662	52586341	GWAS	T	C	2642	2097	0.570	0.531	9.09E-05	1.178	0.042	1.085	1.279		*LOC643714*	0
16	rs3803662	52586341	Rep	T	C	2880	3392	0.572	0.517	4.69E-08	1.245	0.040	1.151	1.347			
16	rs3803662	52586341	Combined	T	C	5522	5489	0.571	0.522	2.79E-11	1.213	0.029	1.146	1.284	3.40E-01		

CHR: chromosome, SNP: single nucleotide polymorphism, BP: SNP genomic location, RA: Risk allele, NRA: Non-risk allele, NCASES: Number of cases, NCONTROLS: Number of controls, RAF: risk allele frequency, P_value: *P*-value from logistic regression analysis after age adjustment, OR: odds ratio, L95: lower 95% confidence interval, U95: upper 95% confidence interval, P_hetero: heterogeneity test with Cochran Q-test, rel.loci: distance of the SNP from the gene, GWAS: genome-wide association study, Rep: validation study.

doi:10.1371/journal.pone.0076463.t002

generated using Locus Zoom (http://csg.sph.umich.edu/locuszoom/).

Weighted genetic risk score (wGRS)

To evaluate the cumulative effects of genetic variants associated with breast cancer risk, we conducted weighted genetic risk score (wGRS) analysis on the basis of genotypes of five SNPs, three significant SNPs (rs2981578 of 10q26/*FGFR2*, rs3803662 and rs12922061 of 16q12/*TOX3*) from this study and two SNPs (rs6557161 of 6q25/*ESR1* and rs10509168 of 10q21/*ZNF365*) that were reported to be associated with breast cancer risk in East Asian population and indicated suggestive association in this study. The wGRS model was developed by logistic regression analysis by incorporating five associated-SNPs and age (as covariates) using GWAS dataset to obtain the estimates (weight) of each corresponding SNP. This model was subsequently validated in an independent samples dataset drawn from the validation phase of this study. The cumulative genetic risk scores were determined by multiplying the number of risk alleles (0/1/2) of an individual by its corresponding weight, and subsequently the sum across the total number of SNPs were taken into consideration. We then classified the genetic risk score into five different categories created from the mean and standard deviation (SD); group 1, < mean-1SD; group 2, mean-1SD to mean; group 3, mean to mean+1SD; group 4, mean+1SD to mean+2SD, group 5, > mean+2SD. Odds ratio and 95% confidence interval were calculated using group 1 as a reference.

Results

In this study, we genotyped a total of 2,725 cases and 2,311 controls with Illumina OmniExpress BeadChip Kits that contained 733,202 SNPs to identify genetic variants associated with the susceptibility to breast cancer in the Japanese population. After quality check of the SNP genotyping data, a total of 550,026 autosomal SNPs were examined for the association by logistic regression analysis. Quantile-quantile (Q-Q) plot and the genomic inflation factor (λ) of the test statistic of this GWAS based on 550, 026 SNPs with all samples was 1.183 suggesting the existence of some population substructure (Figure S2a). To exclude the possibility of population substructure for our sample population, we performed principal component analysis (PCA). Although all the subjects participating in this study were clustered in the Asian population, there was a small portion of samples that were separated from the major Japanese (Hondo) cluster when PCA analysis was performed using only the genotype information of the case and control in the study (Figure S1a and S1b). We then used samples from the major Japanese (Hondo) cluster consisting of 2,642 cases and 2,099 controls, and found that the λ-value improved to 1.027 (Figure S2b). Hence, subsequent analysis was carried out using only samples from the major Japanese cluster. Whole genome imputation utilizing 1000G database as reference panel successfully estimated 7,791,127 SNPs. After stringent quality control by excluding SNPs with r^2-value of <0.9, the total number of SNPs that were taken into account was 5,335,291. The Manhattan plot, plotting $-\log_{10}$ (*P*-value) from the GWAS and imputation analysis against the chromosome position, showed that there were no genetic loci achieving genome-wide significance with the threshold *P*-value of $<5\times10^{-8}$ (Figure 1).

To identify additional susceptible loci associated with breast cancer, we conducted a validation study of 13 genetic loci showing suggestive association ($P<1\times10^{-5}$) with breast cancer after excluding SNPs that showed linkage disequilibrium (LD) coefficient (r^2) of >0.8 within each LD block by examining an

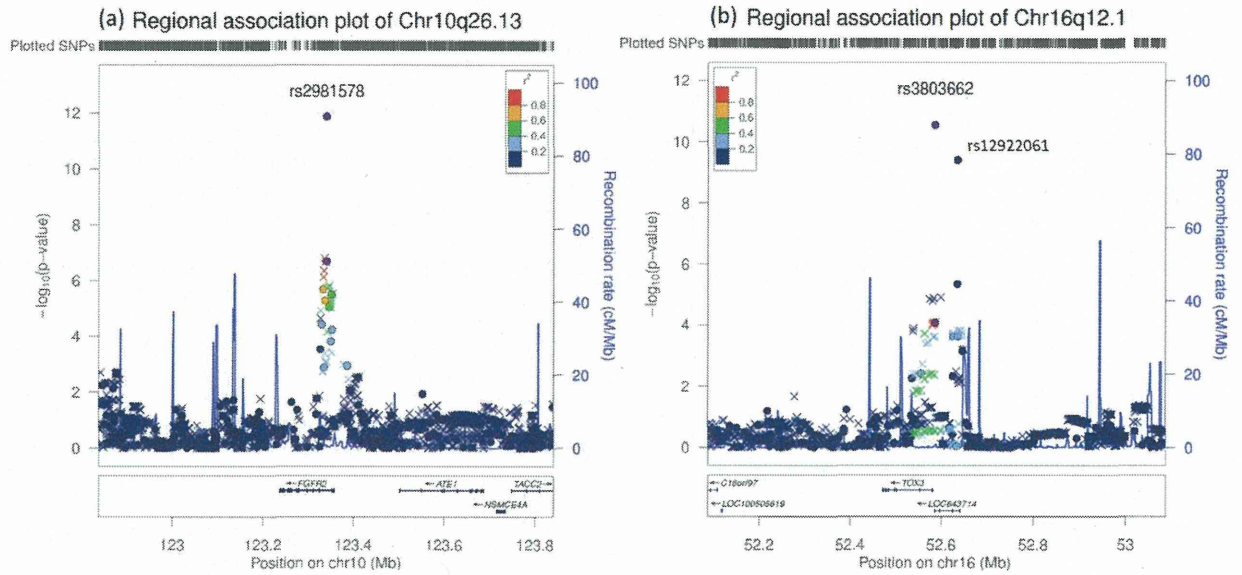

Figure 2. Regional association plots for two significantly associated loci with breast cancer in Japanese population, (a) chromosome 10q26.13 (*FGFR2*) and (b) chromosome 16q21.1 (*TOX3-LOC643714*). SNPs from the GWAS are plotted as circles; imputed SNPs are plotted as crosses. The color intensity reflects the extent of LD with the marker SNP: red, ($r^2 \geq 0.8$), orange ($0.6 \leq r^2 \leq 0.8$), green ($0.4 \leq r^2 \leq 0.6$), light blue ($0.2 \leq r^2 \leq 0.4$) and dark blue ($r^2 < 0.2$). Purplish blue lines represent local recombination rates. The SNP position is based on NCBI build 37.
doi:10.1371/journal.pone.0076463.g002

independent set of 2,885 breast cancer cases and 3,395 controls. Among the 13 loci tested, three SNPs (rs2981578 on chromosome 10q26.13 and rs3803662 along with rs12922061 on chromosome 16q12.1) were successfully validated with Bonferroni-corrected *P*-value of $<3.85\times10^{-3}$ (0.05/13 independent tests) as shown in Table 2 and Table S1. Inverse variance meta-analysis indicated that these three SNPs surpass genome-wide significance level (*P*-value$<5\times10^{-8}$) after combining the GWAS and the validation study with no significant heterogeneity (*P*-value >0.05) between the two stages (Table 2).

The most significantly associated SNP, rs2981578 (combined *P*-value of 1.31×10^{-12}, OR = 1.23; 95% CI = 1.16–.30), is located within the second intron of the *FGFR2* gene on chromosome 10q26.13 (Table 2 and Figure 2a). Variants on this gene have been the most frequently validated to be associated with breast cancer in multiple populations. For chromosome 16q21.1, we successfully validated rs12922061 (combined *P*-value of 3.97×10^{-10}, OR = 1.23; 95% CI = 1.15–.31) to be significantly associated with breast cancer (Table 2 and Figure 2b). After conditioning the effect of rs12922061, rs3803662 remained suggestively associated and was successfully validated after additional samples with a combined *P*-value of 2.79×10^{-11} (OR = 1.21; 95% CI = 1.14–.25). Two of these SNPs remained significant (*P*-value<0.0001) after performing condition analysis by using one of the SNP as covariate, suggesting the independency of association with breast cancer (Table S2). Additionally, the r^2 value between these two SNPs is only 0.17, indicating they are not closely linked with each other. Haplotype analysis of the two SNPs did not reveal stronger association than a single SNP association after 100,000 permutation analysis (Table S3). The SNP, rs3803662, is located in the last exon of *LOC643714* and near to the 5′ end of *TOX3*; whilst rs12922061 is located in the first intron of *LOC643714*.

In addition to perform GWAS for breast cancer in Japanese population, we also evaluated the association of previously-reported breast cancer risk loci in the European and East Asian populations. We evaluated a total of 61 SNPs after excluding 6 SNPs that are not polymorphic in Japanese population (Table S4). Among the 61 SNPs, eight SNPs (rs4415084 of 5p12/*MRPS30*, rs6557161 of 6q25/*ESR1*, rs7465364 of 8p21/*RPL17p33*, rs672888 of 8q24/*MYC*, rs10509168 of 10q21/*ZNF365*, rs1219648 of 10q26/*FGFR2*, rs17221259 of 12p13/*ATF7IP* and rs3803662 of 16q12/*TOX3*) showed suggestive association (*P*-value<0.05) with breast cancer in Japanese population (Table 3). All of these suggestively-associated SNPs possessed the same risk allele and showed the same direction of association that was indicated in the previous reports.

After developing wGRS model using five SNPs from the GWAS dataset, the model was subsequently validated in an independent sample set represented by the validation samples. The cumulative effect of five SNPs evaluated by the wGRS analysis indicated that odds ratio of each category increased according to the level of risk score, and individuals who are in category five carrying the most risk alleles have 2.2 times higher risk to develop breast cancer when utilizing category 1 as a reference (Table 4).

Table 3. Association of previously reported to be breast cancer susceptibility loci in current Japanese GWAS dataset.

CHR	SNP	Chr.loci/Gene	BP	Risk allele	Ref. allele	Case_N	Ctrl_N	RAF_Case	RAF_Ctrl	P-value	OR	SE	L95	U95	Remarks	Reference
5	rs4415084	5p12/*MRPS30*	44662515	T	C	2642	2098	0.601	0.573	8.68E-03	1.118	0.043	1.029	1.215		[27]
6	rs6557161	6q25/*ESR1*	151950235	G	A	2642	2099	0.316	0.286	1.17E-03	1.160	0.046	1.061	1.269	$r^2 = 1.000$ with rs2046210	[22]
8	rs7465364	8p21/*RPL17P33*	29505165	A	G	2641	2099	0.344	0.325	4.91E-02	1.091	0.044	1.000	1.191	$r^2 = 0.961$ with rs9693444	[32]
8	rs672888	8q24/*MYC*	128345463	G	A	2642	2099	0.540	0.516	1.97E-02	1.102	0.042	1.016	1.195	$r^2 = 0.858$ with rs13281615	[18]
10	rs10509168	10q21/*ZNF365*	64257828	G	A	2642	2099	0.484	0.461	2.49E-02	1.099	0.042	1.012	1.193	$r^2 = 0.863$ with rs10822013	[28]
10	rs1219648	10q26/*FGFR2*	123346190	C	T	2641	2099	0.405	0.360	9.85E-06	1.208	0.043	1.111	1.314		[18,19,23,25,33,34]
12	rs17221259	12p13/*ATF7IP*	14410485	G	A	2641	2099	0.243	0.204	6.68E-06	1.252	0.050	1.136	1.381	$r^2 = 0.744$ with rs12422552	[32]
16	rs3803662	16q12/*TOX3*	52586341	T	C	2642	2097	0.570	0.531	9.09E-05	1.178	0.042	1.085	1.279		[18,20,23,25,27]

CHR: chromosome, SNP: single nucleotide polymorphism, Chr.loci/Gene: Chromosome location/Gene, BP: SNP genomic location, Ref: reference, Case_N: Number of cases, Ctrl_N: Number of controls, RAF: risk allele frequency, P_value: *P*-value from logistic regression analysis after age adjustment, OR: odds ratio, L95: lower 95% confidence interval, U95: upper 95% confidence interval.

doi:10.1371/journal.pone.0076463.t003

Discussion

To investigate the involvement of common genetic variants (SNPs) associated with breast cancer in the Japanese population, we performed GWAS, whole genome imputation using 1000G database as reference panel and validation study using a total of 5,527 breast cancer cases and 5,494 controls individuals. We successfully validated the association of chromosome 10q26.13 (*FGFR2*), and 16q12.1 (*TOX3-LOC643714*). In addition to the two aforementioned loci, we validated a total of 67 loci that were previously reported the association with breast cancer and identified six additional loci (rs4415084 of 5p12/*MRPS30*, rs6557161 of 6q25/*ESR1*, rs7465364 of 8p21/*RPL17p33*, rs672888 of 8q24/*MYC*, rs10509168 of 10q21/*ZNF365* and rs17221259 of 12p13/*ATF7IP*) to have suggestive association ($P<0.05$) with breast cancer in Japanese population. Further fine mapping of these loci might identify insightful findings for future analysis.

Hunter DJ *et al.* first reported the association of *FGFR2* with breast cancer in 2007 [19]. Since then, this locus has been successfully validated in various populations throughout the world including those of European ancestry, Asian, Ashkenazi Jewish and Israeli populations [18,37–39]. *FGFR2* encodes fibroblast growth factor receptor type 2, which is a receptor tyrosine kinase playing a critical role in the growth signaling pathway that is involved in growth and differentiation of cells in various tissues including the breast and kidney [40,41]. All the SNPs that were found to be associated with breast cancer are located in intron 2 of the gene; the risk allele of rs2981578, a SNP that was identified in this study, created a putative binding site for Oct-1/Runx2, which gives rise to a strong protein-DNA complex that alters binding of the transcription factor and causes differential expression between the common and minor haplotypes of *FGFR2* [42]. Additionally, Zhu et al. also reported that there is a potential role of histone 3/4 acetylation in modulating access to the polymorphic sites within intron 2 in addition to downstream splicing sites in generating variable FGFR2 levels and isoforms in breast cancer [43].

The second significantly associated locus is located on chromosome 16q12.1 (*TOX3-LOC643714*). *LOC643714* is an uncharacterized gene of unknown function; *TOX3*, also known as *TNRC9* or *CAGF9*, encodes a high mobility group box nuclear protein, which is involved in regulating calcium-dependent transcription [44]. A previous study indicated that increased expression of TOX3 could be a predictor of breast cancer metastasis to bone [45]. In this study, we identified two independently associated SNPs, rs3803662 and rs12922061, with breast cancer in the Japanese population. The minor allele of rs3803662 is reported to cause lower mRNA expression of *TOX3* gene, and this regulatory SNP may alter the expression of a distant gene, *RBL2*, in *cis* [46].

Although wGRS of five associated loci with breast cancer in the Japanese population revealed that individuals with the highest risk (category 5) have 2.2 times higher risk than those with the lowest risk (category 1), it is believed that a complex disease such as breast cancer would be affected by a large number of common genetic variants that have very modest effects. This phenomenon was also supported by the six additional reported loci that showed suggestive association in this dataset, indicating that our current dataset is still under statistical power. Hence, to increase the power and to enlarge the sample number, there is a need for more local and international institutions to collaborate with each other in identifying more common variants associated with breast cancer, which hopefully will lead to the development of promising and accurate prediction system.

Table 4. wGRS using 5 significant associated SNPs evaluated on independent validation sample set.

Category	Case (N = 2869)	Control (N = 3385)	%_Case	%_Ctrl	OR	95%_CI
1	386	676	0.135	0.200	REF	
2	937	1203	0.327	0.355	1.364	1.172–.587
3	998	1056	0.348	0.312	1.655	1.422–.927
4	464	382	0.162	0.113	2.127	1.769–.558
5	84	68	0.029	0.020	2.163	1.535–.050

doi:10.1371/journal.pone.0076463.t004

Supporting Information

Figure S1 Principal component analysis of (a) Case and control samples of this study with four reference populations from the HapMap database which include Europeans (represented by Caucasian from UTAH, CEU), Africans (represented by Yoruba from Ibadan, YRI) and East Asians (represented by Japanese from Tokyo, JPT, and Han Chinese from Beijing, CHB). (b) Case and control samples of this study. Samples from the major cluster (within the black oval circle) were selected for further analysis.
(TIFF)

Figure S2 Quantile-quantile (Q-Q) plot for GWAS of breast cancer in Japanese population with (a) All samples ($\lambda = 1.18$) and (b) Major Japanese (Hondo) cluster ($\lambda = 1.03$).
(TIFF)

Table S1 Association study of the 13 selected loci.
(XLS)

Table S2 Conditioning analysis of SNPs on chromosome 16q12.1.
(XLS)

Table S3 Haplotype analysis and association of SNPs on chromosome 16q12.1.
(XLS)

Table S4 Association study of previously reported breast cancer associated loci.
(XLS)

Acknowledgments

We express our heartfelt gratitude to all the patients who participate in this study. We also thank the members of The Rotary Club of Osaka-Midosuji District 2660 Rotary International in Japan for making this study possible. We would like to express our gratefulness to the staff from Biobank Japan for their outstanding assistance. We extend our appreciation to Mr. Kohei Tomizuka for his insightful comment and members from the Laboratory for Genotyping Development, Center for Integrative Medical Sciences, RIKEN for their technical support.

Author Contributions

Conceived and designed the experiments: YN TK. Performed the experiments: SKL KA. Analyzed the data: SKL AT. Contributed reagents/materials/analysis tools: AT JI YM MK. Wrote the paper: SKL YN TK.

References

1. Phipps AI, Chlebowski RT, Prentice R, McTiernan A, Wactawski-Wende J, et al. (2011) Reproductive history and oral contraceptive use in relation to risk of triple-negative breast cancer. J Natl Cancer Inst 103: 470–77.
2. Iodice S, Barile M, Rotmensz N, Feroce I, Bonanni B, et al. (2010) Oral contraceptive use and breast or ovarian cancer risk in BRCA1/2 carriers: a meta-analysis. Eur J Cancer 46: 2275–284.
3. Anderson GL, Limacher M, Assaf AR, Bassford T, Beresford SA, et al. (2004) Effects of conjugated equine estrogen in postmenopausal women with hysterectomy: the Women's Health Initiative randomized controlled trial. JAMA 291: 1701–712.
4. Hamajima N, Hirose K, Tajima K, Rohan T, Calle EE, et al. (2002) Alcohol, tobacco and breast cancer – llaborative reanalysis of individual data from 53 epidemiological studies, including 58,515 women with breast cancer and 95,067 women without the disease. Br J Cancer 87: 1234–245.
5. McTiernan A (2003) Behavioral risk factors in breast cancer: can risk be modified? Oncologist 8: 326–334.
6. Islam T, Ito H, Sueta A, Hosono S, Hirose K, et al. (2012) Alcohol and dietary folate intake and the risk of breast cancer: a case-control study in Japan. Eur J Cancer Prev.
7. Chen J, Pee D, Ayyagari R, Graubard B, Schairer C, et al. (2006) Projecting absolute invasive breast cancer risk in white women with a model that includes mammographic density. J Natl Cancer Inst 98: 1215–1226.
8. Pharoah PD, Day NE, Duffy S, Easton DF, Ponder BA (1997) Family history and the risk of breast cancer: a systematic review and meta-analysis. Int J Cancer 71: 800–809.
9. Miki Y, Swensen J, Shattuck-Eidens D, Futreal PA, Harshman K, et al. (1994) A strong candidate for the breast and ovarian cancer susceptibility gene BRCA1. Science 266: 66–71.
10. Wooster R, Bignell G, Lancaster J, Swift S, Seal S, et al. (1995) Identification of the breast cancer susceptibility gene BRCA2. Nature 378: 789–792.
11. Renwick A, Thompson D, Seal S, Kelly P, Chagtai T, et al. (2006) ATM mutations that cause ataxia-telangiectasia are breast cancer susceptibility alleles. Nat Genet 38: 873–875.
12. Coles C, Condie A, Chetty U, Steel CM, Evans HJ, et al. (1992) p53 mutations in breast cancer. Cancer Res 52: 5291–5298.
13. Consortium CBCC-C (2004) CHEK2*1100delC and susceptibility to breast cancer: a collaborative analysis involving 10,860 breast cancer cases and 9,065 controls from 10 studies. Am J Hum Genet 74: 1175–1182.
14. Liaw D, Marsh DJ, Li J, Dahia PL, Wang SI, et al. (1997) Germline mutations of the PTEN gene in Cowden disease, an inherited breast and thyroid cancer syndrome. Nat Genet 16: 64–67.
15. Berx G, Cleton-Jansen AM, Nollet F, de Leeuw WJ, van de Vijver M, et al. (1995) E-cadherin is a tumour/invasion suppressor gene mutated in human lobular breast cancers. EMBO J 14: 6107–6115.
16. Hearle N, Schumacher V, Menko FH, Olschwang S, Boardman LA, et al. (2006) Frequency and spectrum of cancers in the Peutz-Jeghers syndrome. Clin Cancer Res 12: 3209–3215.
17. Hofstatter EW, Domchek SM, Miron A, Garber J, Wang M, et al. (2011) PALB2 mutations in familial breast and pancreatic cancer. Fam Cancer 10: 225–231.
18. Easton DF, Pooley KA, Dunning AM, Pharoah PD, Thompson D, et al. (2007) Genome-wide association study identifies novel breast cancer susceptibility loci. Nature 447: 1087–1093.
19. Hunter DJ, Kraft P, Jacobs KB, Cox DG, Yeager M, et al. (2007) A genome-wide association study identifies alleles in FGFR2 associated with risk of sporadic postmenopausal breast cancer. Nat Genet 39: 870–874.
20. Stacey SN, Manolescu A, Sulem P, Rafnar T, Gudmundsson J, et al. (2007) Common variants on chromosomes 2q35 and 16q12 confer susceptibility to estrogen receptor-positive breast cancer. Nat Genet 39: 865–869.
21. Stacey SN, Manolescu A, Sulem P, Thorlacius S, Gudjonsson SA, et al. (2008) Common variants on chromosome 5p12 confer susceptibility to estrogen receptor-positive breast cancer. Nat Genet 40: 703–706.
22. Zheng W, Long J, Gao YT, Li C, Zheng Y, et al. (2009) Genome-wide association study identifies a new breast cancer susceptibility locus at 6q25.1. Nat Genet 41: 324–328.

23. Thomas G, Jacobs KB, Kraft P, Yeager M, Wacholder S, et al. (2009) A multistage genome-wide association study in breast cancer identifies two new risk alleles at 1p11.2 and 14q24.1 (RAD51L1). Nat Genet 41: 579–584.
24. Ahmed S, Thomas G, Ghoussaini M, Healey CS, Humphreys MK, et al. (2009) Newly discovered breast cancer susceptibility loci on 3p24 and 17q23.2. Nat Genet 41: 585–590.
25. Turnbull C, Ahmed S, Morrison J, Pernet D, Renwick A, et al. (2010) Genome-wide association study identifies five new breast cancer susceptibility loci. Nat Genet 42: 504–507.
26. Long J, Cai Q, Shu XO, Qu S, Li C, et al. (2010) Identification of a functional genetic variant at 16q12.1 for breast cancer risk: results from the Asia Breast Cancer Consortium. PLoS Genet 6: e1001002.
27. Fletcher O, Johnson N, Orr N, Hosking FJ, Gibson LJ, et al. (2011) Novel breast cancer susceptibility locus at 9q31.2: results of a genome-wide association study. J Natl Cancer Inst 103: 425–435.
28. Cai Q, Long J, Lu W, Qu S, Wen W, et al. (2011) Genome-wide association study identifies breast cancer risk variant at 10q21.2: results from the Asia Breast Cancer Consortium. Hum Mol Genet 20: 4991–4999.
29. Long J, Cai Q, Sung H, Shi J, Zhang B, et al. (2012) Genome-wide association study in east Asians identifies novel susceptibility loci for breast cancer. PLoS Genet 8: e1002532.
30. Ghoussaini M, Fletcher O, Michailidou K, Turnbull C, Schmidt MK, et al. (2012) Genome-wide association analysis identifies three new breast cancer susceptibility loci. Nat Genet 44: 312–318.
31. Lindstrom S, Vachon CM, Li J, Varghese J, Thompson D, et al. (2011) Common variants in ZNF365 are associated with both mammographic density and breast cancer risk. Nat Genet 43: 185–187.
32. Michailidou K, Hall P, Gonzalez-Neira A, Ghoussaini M, Dennis J, et al. (2013) Large-scale genotyping identifies 41 new loci associated with breast cancer risk. Nat Genet 45: 353–361, 361e351–352.
33. Li J, Humphreys K, Heikkinen T, Aittomaki K, Blomqvist C, et al. (2011) A combined analysis of genome-wide association studies in breast cancer. Breast Cancer Res Treat 126: 717–727.
34. Haiman CA, Chen GK, Vachon CM, Canzian F, Dunning A, et al. (2011) A common variant at the TERT-CLPTM1L locus is associated with estrogen receptor-negative breast cancer. Nat Genet 43: 1210–1214.
35. Elgazzar S, Zembutsu H, Takahashi A, Kubo M, Aki F, et al. (2012) A genome-wide association study identifies a genetic variant in the SIAH2 locus associated with hormonal receptor-positive breast cancer in Japanese. J Hum Genet 57: 766–771.
36. Ohnishi Y, Tanaka T, Ozaki K, Yamada R, Suzuki H, et al. (2001) A high-throughput SNP typing system for genome-wide association studies. J Hum Genet 46: 471–477.
37. Liang J, Chen P, Hu Z, Zhou X, Chen L, et al. (2008) Genetic variants in fibroblast growth factor receptor 2 (FGFR2) contribute to susceptibility of breast cancer in Chinese women. Carcinogenesis 29: 2341–2346.
38. Gold B, Kirchhoff T, Stefanov S, Lautenberger J, Viale A, et al. (2008) Genome-wide association study provides evidence for a breast cancer risk locus at 6q22.33. Proc Natl Acad Sci U S A 105: 4340–4345.
39. Raskin L, Pinchev M, Arad C, Lejbkowicz F, Tamir A, et al. (2008) FGFR2 is a breast cancer susceptibility gene in Jewish and Arab Israeli populations. Cancer Epidemiol Biomarkers Prev 17: 1060–1065.
40. Bates CM (2007) Role of fibroblast growth factor receptor signaling in kidney development. Pediatr Nephrol 22: 343–349.
41. Parsa S, Ramasamy SK, De Langhe S, Gupte VV, Haigh JJ, et al. (2008) Terminal end bud maintenance in mammary gland is dependent upon FGFR2b signaling. Dev Biol 317: 121–131.
42. Meyer KB, Maia AT, O'Reilly M, Teschendorff AE, Chin SF, et al. (2008) Allele-specific up-regulation of FGFR2 increases susceptibility to breast cancer. PLoS Biol 6: e108.
43. Zhu X, Asa SL, Ezzat S (2009) Histone-acetylated control of fibroblast growth factor receptor 2 intron 2 polymorphisms and isoform splicing in breast cancer. Mol Endocrinol 23: 1397–1405.
44. Yuan SH, Qiu Z, Ghosh A (2009) TOX3 regulates calcium-dependent transcription in neurons. Proc Natl Acad Sci U S A 106: 2909–2914.
45. Smid M, Wang Y, Klijn JG, Sieuwerts AM, Zhang Y, et al. (2006) Genes associated with breast cancer metastatic to bone. J Clin Oncol 24: 2261–2267.
46. Gudmundsdottir ET, Barkardottir RB, Arason A, Gunnarsson H, Amundadottir LT, et al. (2012) The risk allele of SNP rs3803662 and the mRNA level of its closest genes TOX3 and LOC643714 predict adverse outcome for breast cancer patients. BMC Cancer 12: 621.

nature COMMUNICATIONS

ARTICLE

Received 2 Feb 2013 | Accepted 15 Aug 2013 | Published 20 Sep 2013

DOI: 10.1038/ncomms3443 OPEN

Targeting BIG3–PHB2 interaction to overcome tamoxifen resistance in breast cancer cells

Tetsuro Yoshimaru[1], Masato Komatsu[1], Taisuke Matsuo[1], Yi-An Chen[2], Yoichi Murakami[2,†], Kenji Mizuguchi[2], Eiichi Mizohata[3], Tsuyoshi Inoue[3], Miki Akiyama[4], Rui Yamaguchi[5], Seiya Imoto[6], Satoru Miyano[6], Yasuo Miyoshi[7], Mitsunori Sasa[8], Yusuke Nakamura[4,9] & Toyomasa Katagiri[1]

The acquisition of endocrine resistance is a common obstacle in endocrine therapy of patients with oestrogen receptor-α (ERα)-positive breast tumours. We previously demonstrated that the BIG3–PHB2 complex has a crucial role in the modulation of oestrogen/ERα signalling in breast cancer cells. Here we report a cell-permeable peptide inhibitor, called ERAP, that regulates multiple ERα-signalling pathways associated with tamoxifen resistance in breast cancer cells by inhibiting the interaction between BIG3 and PHB2. Intrinsic PHB2 released from BIG3 by ERAP directly binds to both nuclear- and membrane-associated ERα, which leads to the inhibition of multiple ERα-signalling pathways, including genomic and non-genomic ERα activation and ERα phosphorylation, and the growth of ERα-positive breast cancer cells both *in vitro* and *in vivo*. More importantly, ERAP treatment suppresses tamoxifen resistance and enhances tamoxifen responsiveness in ERα-positive breast cancer cells. These findings suggest inhibiting the interaction between BIG3 and PHB2 may be a new therapeutic strategy for the treatment of luminal-type breast cancer.

[1] Division of Genome Medicine, Institute for Genome Research, The University of Tokushima, 3-18-15, Kuramoto-cho, Tokushima 770-8503, Japan. [2] National Institute of Biomedical Innovation, 7-6-8 Asagi-Saito, Ibaraki-City, Osaka 567-0085, Japan. [3] Department of Applied Chemistry, Graduate School of Engineering, Osaka University, 2-1, Yamada-oka, Suita, Osaka 565-0871, Japan. [4] Laboratory of Molecular Medicine, University of Tokyo, 4-6-1, Shirokanedai, Minato-ku, Tokyo 108-8639, Japan. [5] Laboratory of Sequence Analysis, The University of Tokyo, 4-6-1, Shirokanedai, Minato-ku, Tokyo 108-8639, Japan. [6] Laboratory of DNA Information Analysis, Human Genome Centre, Institute of Medical Science, The University of Tokyo, 4-6-1, Shirokanedai, Minato-ku, Tokyo 108-8639, Japan. [7] Division of Breast and Endocrine Surgery, Department of Surgery, Hyogo College of Medicine, 1-1, Mukogawa-cho, Nishinomiya, Hyogo 663-8501, Japan. [8] Department of Surgery, Tokushima Breast Care Clinic, 4-7-7, Nakashimada, Tokushima 770-0052, Japan. [9] Department of Medicine and Surgery, The University of Chicago, 900 E 57th Street, KCBD6126, Chicago, Illinois 60637, USA. † Present address: Graduate School of Information Sciences, Tohoku University, 6-3-09, Aramaki-aza-aoba, Aoba-ku, Sendai-city, Miyagi 980-8579, Japan. Correspondence and requests for materials should be addressed to T.K. (email: tkatagi@genome.tokushima-u.ac.jp).

Breast cancer is the most common cancer among women worldwide[1,2]. More than 70% of primary breast tumours are oestrogen receptor-α (ERα)-positive, and the interactions between oestrogen (E2) and ERα dramatically enhance the proliferative and metastatic activity of breast tumour cells[3,4]. E2 biological actions are mediated by both genomic and non-genomic mechanisms; in the former type nuclear ERα functions as a ligand-dependent transcription factor that regulates target gene expression levels[3,5], whereas in the latter type E2-bound ERα in the plasma membrane associates with a variety of signalling molecules, including IGF receptor β (IGF-1Rβ), phosphoinositide 3-kinase (PI3K) and SH2 domain containing (Shc), which results in Akt and mitogen-activated protein kinase (MAPK) activation or increased nuclear ERα phosphorylation[6–10]. Thus, ERα has a pivotal role in the E2 signalling network and therefore represents an important therapeutic target for breast cancer.

The selective ER modulator tamoxifen directly inhibits E2 and ERα interactions, and is a standard treatment offered to patients with ERα-positive breast cancer[11–13]. Nonetheless, tumours often develop resistance, leaving patients with recurrent tumours that lack targeted therapeutic options[14,15]. The potential mechanisms for either intrinsic or acquired endocrine resistance remain poorly understood, but they clearly include ERα-coregulatory proteins and cross-talk between the ERα pathway and other growth factors and kinase networks[10,11,16]. This knowledge has led to numerous treatment strategies combining endocrine and targeted inhibitor therapies[17–19]; however, comprehensive measures for this problem remain unresolved. Therefore, identifying the factors and pathways responsible for resistance and defining ways to overcome it represent important therapeutic challenges in breast cancer research.

The novel E2/ERα signalling regulator brefeldin A-inhibited guanine nucleotide-exchange protein 3 (BIG3), which is exclusively overexpressed in a majority of breast cancers, was recently identified from genome-wide expression profiles[20,21]. BIG3 interacts and colocalizes with prohibitin 2 (PHB2) in the cytoplasm of breast cancer cells[20,21]. PHB2 is known to function as a corepressor of ERα[22,23]. Our previous study demonstrated that when BIG3 was knocked down by small interfering RNA, E2 stimulation led to the nuclear translocation of a majority of the cytoplasmic PHB2, enhanced the interaction between PHB2 and ERα, and suppressed ERα transcriptional activity[21]. Accordingly, we hypothesized that BIG3 captures PHB2 in the cytoplasm of cancer cells and thereby inhibits the suppressive ability of PHB2 in the presence of E2, resulting in the constitutive activation of ERα signalling pathways.

Here we describe a synthetic, cell-penetrating, dominant-negative peptide that inhibits the E2/ERα signalling network by activating the tumour suppressive ability of PHB2. This peptide also enhanced tamoxifen responsiveness and anti-tumour effects in tamoxifen-resistant (TAM-R) breast cancers. Thus, the regulation of E2 signalling by targeting the BIG3–PHB2 interaction introduces a new potential therapeutic approach for endocrine-resistant tumours, as well as ERα-positive breast cancers.

Results

Identification of the BIG3–PHB2 interacting region. Previous studies have shown that the BIG3–PHB2 complex has a critical role in breast cancer cell growth[21], and strategies capable of inhibiting this interaction may represent novel therapies for breast cancer. Therefore, we first attempted to determine the BIG3 region(s) required for the interaction with PHB2 through *in silico* and biochemical analyses. First, we independently co-transfected five partial constructs of FLAG-tagged BIG3 (Fig. 1a) with HA-tagged PHB2 (HA-PHB2) into COS-7 cells. Immunoprecipitation with an anti-FLAG antibody indicated that HA-PHB2 co-immunoprecipitated with $BIG3_{1-434}$, $BIG3_{1-250}$ and full-length BIG3 (Fig. 1b), suggesting that the 101–250th amino acid region of BIG3 is minimally required for its interaction with PHB2.

In parallel with this approach, we attempted to predict the protein binding sites on BIG3 using the PSIVER (Protein–protein interaction SIte prediction server) software[24], and we identified a cluster of candidate binding residues within the 101–250th amino acid region. This cluster region contained three of the highest scoring (≥ 0.6) residues (Q165, D169 and Q173; Fig. 1c), which were oriented in the same direction (Fig. 1d). Indeed, the BIG3 mutations in which all of these target residues were substituted with alanine almost completely abolished the interaction with HA-PHB2 (Fig. 1e), indicating the importance of Q165, D169 and Q173 for BIG3 heterodimerization with PHB2. Moreover, D169 was the most critical site among these residues for binding, although an alanine mutation on each residue resulted in reduced binding (Supplementary Fig. S1). Accordingly, we focused on these residues as candidate PHB2-binding residues.

A peptide with dominant-negative influence on ERα activity. We next investigated the possibility of a cell-penetrating peptide as a dominant-negative inhibitor targeting the BIG3–PHB2 interaction, and designed a specific peptide that included these PHB2-binding residues to target the BIG3–PHB2 interaction. This peptide, referred to as ERα activity-regulator synthetic peptide (ERAP), contained the BIG3 potential binding residues (165–QMLSDLTLQLRQR–177) and membrane-permeable polyarginine residues (11R) at its NH_2 terminus (Fig. 2a). As negative controls, peptides containing a scrambled amino acid sequence (scrERAP) and either alanine mutations at key residues (mtERAP) were constructed (Fig. 2a). Indeed, co-immunoprecipitation experiments revealed that ERAP, but not mtERAP or scrERAP, completely inhibited the complex formation of endogenous BIG3 and PHB2 in the ERα-positive breast cancer cell lines MCF-7 and KPL-3C, which strongly express BIG3 and PHB2 (Fig. 2b and Supplementary Fig. S2). We also examined the direct inhibition of the BIG3–PHB2 interaction using ERAP. As expected, HA-ERAP bound to His-tagged recombinant PHB2 protein and inhibited the BIG3–PHB2 interaction in a dose-dependent manner, whereas scrERAP did not (Fig. 2c). In addition, mtERAP exhibited modest binding to the PHB2 protein at levels substantially lower than ERAP (Fig. 2c). Surface plasmon resonance (BIAcore) interaction analysis revealed that ERAP bound to the His-tagged recombinant PHB2 with a dissociation constant (Kd) = 18.9 μM (Fig. 2d). Thus, our data suggested that ERAP directly bound to PHB2, resulting in the specific inhibition of BIG3–PHB2 complex formation.

ERAP translocates PHB2 and attenuates nuclear ERα activation. We investigated the subcellular distribution of endogenous PHB2 in breast cancer cells following ERAP treatment by immunocytochemical and biochemical approaches. In the presence of E2, treatment with ERAP, but not with scrERAP, led to a significant increase in the amount of nuclear PHB2 in a time-dependent fashion (Fig. 3a). In addition, in the presence of E2, ERAP treatment led to a decrease in cytoplasmic PHB2, thereby substantially increasing the interaction between PHB2 and ERα in the nucleus even after 1 h (Fig. 3b). Furthermore, ERAP co-immunoprecipitated and colocalized with endogenous PHB2 in the nucleus and the cytoplasm (Supplementary Fig. S3a,b) but did not directly bind to ERα or BIG3. These findings suggested that ERAP caused PHB2 to be released from BIG3 and led to

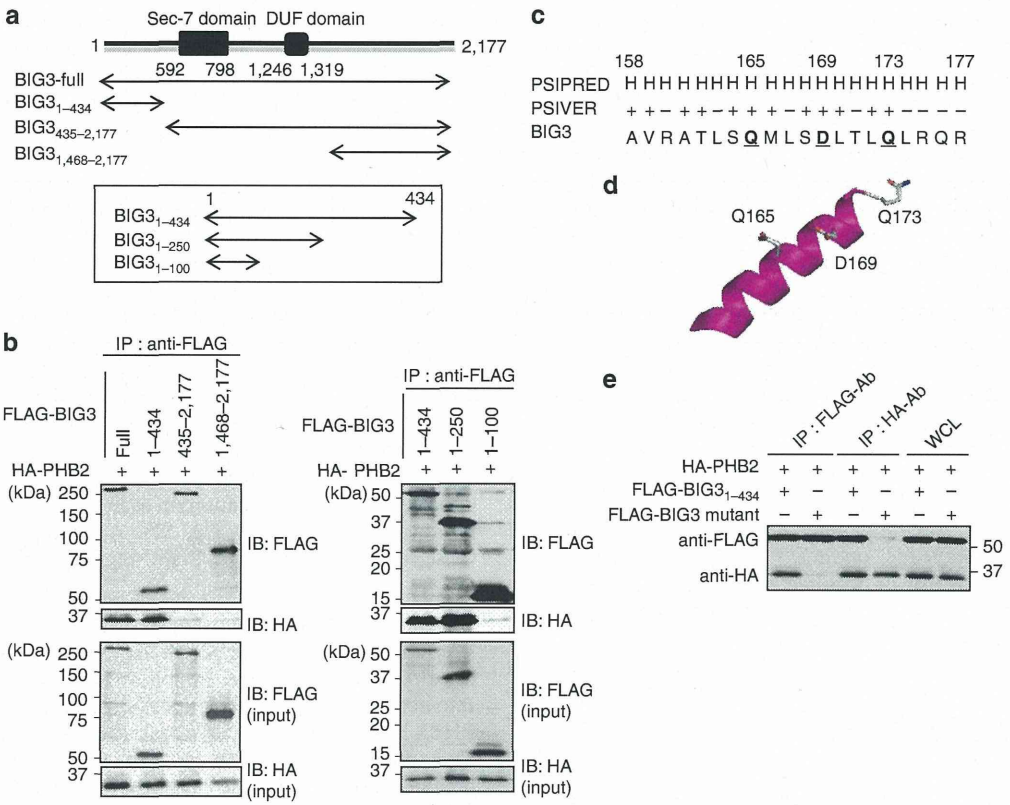

Figure 1 | Identification of the BIG3-PHB2 interacting region. (**a**) The schematic representation of human BIG3 and the five FLAG-BIG3 partial clones lacking one of the terminal regions is shown. (**b**) Immunoblot analyses were performed to identify the PHB2-binding region in BIG3. COS-7 cells were transfected with the indicated BIG3 constructs (full-length BIG3, BIG3$_{1-434}$, BIG3$_{435-2,177}$, BIG3$_{1,468-2177}$, BIG3$_{1-100}$ and BIG3$_{1-250}$) and HA-PHB2. After 48 h, the cells were lysed and FLAG-BIG3 was immunoprecipitated with an anti-FLAG antibody. Immunoprecipitated proteins and a portion of the original cell lysates (input) were immunoblotted as indicated. (**c**) The predicted interaction sites, as determined using PSIVER software, are shown. The underlined bold letters indicate the residues most likely to be involved in BIG3-PHB2 binding. (**d**) The putative PHB2-binding sites (Q165, D169 and Q173) on a predicted three-dimensional structure of BIG3 protein are shown. (**e**) Immunoblots were performed to assess the PHB2-binding region in BIG3 protein. The lysates from COS-7 cells transfected with BIG3$_{1-434}$ or mutant BIG3 constructs were immunoprecipitated with anti-FLAG and anti-HA antibodies to detect BIG3 and PHB2, respectively. Full-length images of immunoblots are shown in Supplementary Fig. S9.

E2-dependent PHB2 nuclear translocation, eventually resulting in the interaction of PHB2 with nuclear ERα in cancer cells.

ERα has been shown to modulate transcription in two ways: (i) through direct binding to oestrogen-responsive elements (EREs) located in the promoter and/or enhancer regions of target genes[25] and (ii) by serving as a co-activator of other transcription factors such as AP-1 (ref. 26). Therefore, we explored the impact of ERAP treatment on these two modes of ERα transcriptional activity. First, we performed a chromatin immunoprecipitation (ChIP) assay with E2-stimulated MCF-7 cells. The results showed that ERAP treatment induced E2-dependent recruitment of the endogenous ERα–PHB2 complex on the ERα target genes, *TFF1* and *CCND1*, respectively, (Fig. 3c), suggesting that ERAP did not inhibit the ability of ERα to bind ERE or AP-1. In luciferase assays with ERE or AP-1 reporters, ERAP significantly inhibited both forms of E2-induced ERα transcriptional activity in a dose-dependent manner in MCF-7 and KPL-3C cells (Supplementary Fig. S3c), but no significant inhibition was observed with scrERAP or mtERAP. These results indicated that ERAP suppressed ERα transcriptional activity levels through both canonical ERE- and non-canonical AP-1-binding mechanisms.

PHB2 is known to act as an ERα transcriptional corepressor by competing with the co-activator SRC-1 to bind ERα[23] and by recruiting histone deacetylase 1 (HDAC1; ref. 27) and another corepressor, NcoR[28]. Thus, we next explored the effect of ERAP on this recruitment in MCF-7 and KPL-3C cells using ChIP assays. Stimulation with E2 alone recruited SRC-1 to ERα, whereas ERAP treatment led to the direct association of PHB2 with ERα in the presence of E2, reduced SRC-1 binding to ERα, and enhanced the recruitment of HDAC1 and NcoR in MCF-7 (Fig. 3d) and KPL-3C cells (Supplementary Fig. S3d). Moreover, we performed a ChIP–quantitative PCR assay, with E2-stimulated MCF-7 cells. The results showed that ERAP treatment significantly reduced the E2-dependent recruitment of endogenous SRC-1 on the *TFF1* gene but increased the E2-dependent recruitment of endogenous NcoR, HDAC1 and PHB2 (Supplementary Fig. S3e). In contrast, ERAP treatment had no effect on ChIP assay using an anti-BIG3 antibody (Supplementary Fig. S3e) or on ERα expression at the mRNA or protein level (Supplementary Fig. S3f). Subsequently, we investigated the HDAC activity of PHB2 immunoprecipitates in MCF-7 cells and found that the chromatin-remodelling complexes recruited by ERAP treatment led to a significant increase in HDAC activity (Fig. 3e). Moreover, ERAP significantly suppressed E2-induced expression of *TFF1*, *CCND1*, *c-Myc*, *E2F1* and *PgR*[29–33] (Fig. 3f). In addition, we validated the suppressive effect of BIG3 on ERα transcriptional activity. BIG3

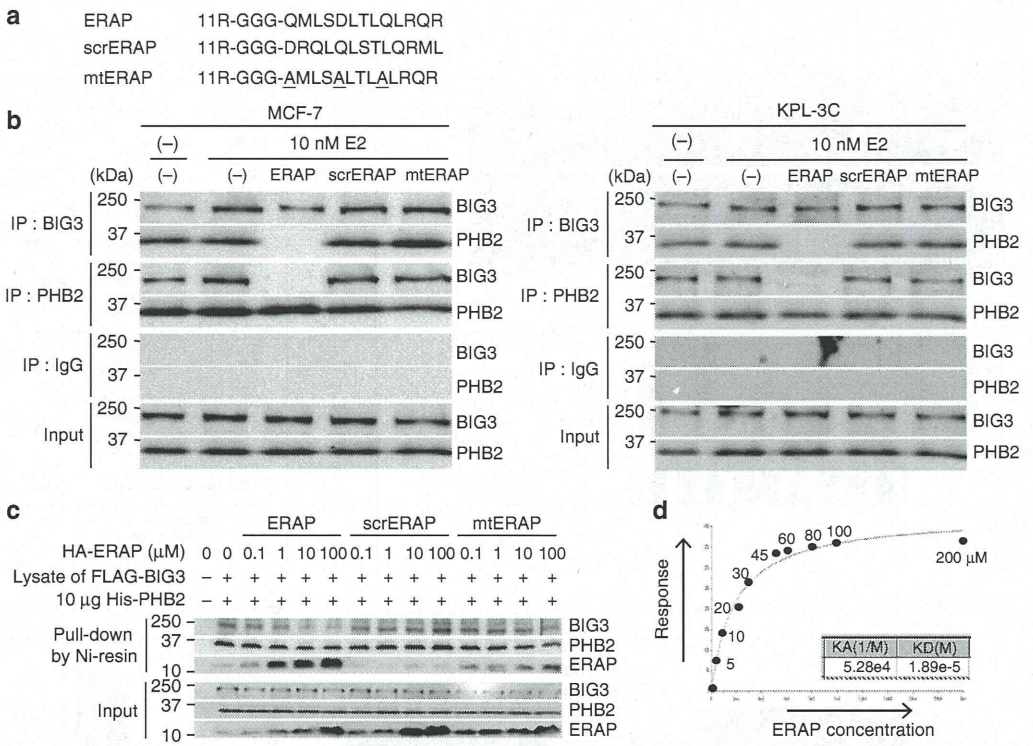

Figure 2 | ERAP inhibits the interaction of BIG3 with PHB2. (**a**) The ERAP, scrERAP and mtERAP sequences are shown. (**b**) The inhibitory effects of ERAP treatment on BIG3–PHB2 interactions were evaluated in MCF-7 (left) and KPL-3C cells (right). (**c**) Direct inhibition of the BIG3–PHB2 interaction by ERAP was evaluated. The lysates of COS-7 cells, transiently transfected with FLAG-BIG3, were incubated with 6 × His-tagged recombinant PHB2 (His-PHB2) and HA-ERAP, HA-scrERAP or HA-mtERAP for 1 h. Then, His-PHB2 was captured with Ni-NTA agarose, and the bound fractions were immunoblotted as indicated. (**d**) *In vitro* direct interaction of ERAP and PHB2 was evaluated by BIAcore.

depletion caused a significant reduction in the canonical ERE and non-canonical AP-1 ERα transcriptional activities in ERα-positive MCF-7 cells but did not affect ERα-negative MDA-MB-231 cells (Supplementary Fig. S3g). Taken together, these findings indicated that nuclear-translocated PHB2 following ERAP treatment directly bound to ERα and acted as a corepressor by recruiting HDAC1 and NcoR, thereby leading to an almost complete suppression of the ERα target gene expression.

ERAP suppresses E2-dependent non-genomic ERα signalling. In addition to ERα acting as a nuclear transcription factor, E2 rapidly induces IGF-1Rβ tyrosine phosphorylation followed by the formation of a ternary complex of IGF-1Rβ, ERα and Shc in the cell membrane[9], even though the abundance of membrane-bound and cytoplasmic ERα is low in primary breast cancers[34]. Indeed, we observed that a portion of PHB2 released from BIG3 by ERAP interacted with ERα in the cytoplasmic/plasma membrane cell fraction, regardless of the presence of E2 (Fig. 3a,b and Supplementary Fig. S3a,b). Therefore, we hypothesized that ERAP could also affect these non-genomic actions of ERα. First, we detected E2-induced tyrosine phosphorylation of IGF-1Rβ and co-immunoprecipitated IGF-1Rβ, ERα and Shc in both MCF-7 and KLP-3C cells (Fig. 4a), which highly expressed IGF-1Rβ and PI3K (Supplementary Fig. S4a), as described previously[9]. In contrast, ERAP treatment removed Shc from this complex and formed a new ternary complex consisting of IGF-1Rβ, ERα and PHB2, and thereby suppressed E2-induced tyrosine phosphorylation of IGF-1Rβ (Fig. 4a). We then examined the effects of ERAP on the phosphorylation of membrane-associated ERα (S118), because its phosphorylation has been associated with invasive breast cancer in clinical specimens[35]. ERAP treatment clearly suppressed the E2-induced phosphorylation (S118) of membrane-associated ERα in the IGF-1Rβ-precipitated membrane fraction of MCF-7 cells (Supplementary Fig. S4b). Moreover, ERAP also interfered with the E2-induced interactions of ERα and PI3K in both MCF-7 and KLP-3C cells (Fig. 4b). Next, we examined the effects of ERAP on the phosphorylation status of Akt and p42/44 MAPK, which are the downstream signalling molecules of IGF-1Rβ and PI3K, respectively. As expected, we observed that Akt (S473) and p42/44 MAPK (T202/Y204) phosphorylation levels were clearly increased in a time-dependent manner after E2 stimulation in both cell lines, whereas treatment with ERAP, but not scrERAP, completely suppressed the E2-induced phosphorylation levels of both proteins (Fig. 4c and Supplementary Fig. S4c). However, the PHB2 released from BIG3 following ERAP treatment did not directly interact with Akt or p42/44 MAPK (Supplementary Fig. S4d). Taken together, these results strongly suggested that ERAP interfered with E2-induced non-genomic ERα activation pathways, such as those mediated by IGF-1Rβ.

ERAP represses E2-dependent ERα phosphorylation. Accumulating evidence suggests that phosphorylation of ERα is an important regulator of E2-induced ERα transcriptional activity, DNA-binding, co-activator binding, and protein stability and cell proliferation in ERα-positive breast cancer cells[36–43]. Thus, we examined the effects of ERAP on ERα phosphorylation at sites, including S104/S106, S118, S167, S305 and Y537.